HHS Public Access

Author manuscript

Nat Neurosci. Author manuscript; available in PMC 2010 April 01.

Published in final edited form as:

Nat Neurosci. 2009 October ; 12(10): 1275–1284. doi:10.1038/nn.2386.

Epac2 induces synapse remodeling and depression and its disease-associated forms alter spine morphology

Kevin M. Woolfrey[1,*], **Deepak P. Srivastava**[1,*], **Huzefa Photowala**[1], **Megumi Yamashita**[2], **Maria V. Barbolina**[3], **Michael E. Cahill**[1], **Zhong Xie**[1], **Kelly A. Jones**[1], **Lawrence A. Quilliam**[4], **Murali Prakriya**[2], and **Peter Penzes**[1,§]

[1]Department of Physiology, Northwestern University Feinberg School of Medicine, 303 E. Chicago Avenue, Chicago, IL 60611.

[2]Department of Molecular Pharmacology and Biological Chemistry, Northwestern University Feinberg School of Medicine, 303 E. Chicago Avenue, Chicago, IL 60611.

[3]Department of Biopharmaceutical Sciences, University of Illinois, 833 South Wood Street, Chicago, IL 60612.

[4]Department of Biochemistry and Molecular Biology, Indiana University School of Medicine and Walther Cancer Institute, 635 Barnhill Drive, Indianapolis, IN 46202.

Abstract

Dynamic remodeling of spiny synapses is crucial for cortical circuit development, refinement, and plasticity, while abnormal morphogenesis is associated with neuropsychiatric disorders. Here we show in cultured rat cortical neurons that activation of Epac2, a PKA-independent cAMP target and Rap guanine-nucleotide exchange factor (GEF), induces spine shrinkage, increases spine motility, removes synaptic GluR2/3-containing AMPA receptors, and depresses excitatory transmission, while its inhibition promotes spine enlargement and stabilization. Epac2 is required for dopamine D1-like receptor-dependent spine shrinkage and GluR2 removal from spines. Epac2 interaction with neuroligin promotes its membrane recruitment and enhances its GEF activity. Rare missense mutations in the *EPAC2* gene, previously found in individuals with autism, affect basal and neuroligin-stimulated GEF activity, dendritic Rap signaling, synaptic protein distribution, and spine morphology. Thus, we identify a novel mechanism that promotes dynamic remodeling and depression of spiny synapses, whose mutations may contribute to some aspects of disease.

[§]To whom correspondence should be addressed.

[*]These authors contributed equally to this work

Author contributions

K.M.W. and D.P.S. designed and performed the experiments, H.P., M.V.B., M.E.C., Z.X. and K.A.J. performed experiments, M.Y. and M.P. performed the mEPSC experiments and assisted in data analysis, L.A.Q. contributed reagents and provided technical expertise, K.M.W., D.P.S., and P.P. wrote the manuscript. P.P. directed the project.

Keywords

glutamate receptor; dendritic spine; autism; neuroligin; GEF; Rap; GTPase; GluR2; postsynaptic; cAMP; excitatory synapse; PKA; dopamine

Remodeling of central neural circuits depends on the bidirectional control of synapse stability, structure, and strength. Synapse stabilization, enlargement, and potentiation contribute to the establishment of long-lasting synaptic connections. On the other hand, recent imaging studies suggest that a fraction of spines become thin and small, and display increased motility and turnover1. Such spines have reduced AMPA receptor (AMPAR) content and make weaker synapses2; spine shrinkage is associated with depressed glutamatergic transmission3,4. Synaptic dynamic remodeling thus contributes to neural circuit development, as well as to the experience-dependent refinement and plasticity of brain circuits during critical periods5 and throughout life1. Conversely, abnormal synapse remodeling underlies to many neuropathologies6. However, the mechanisms that actively promote coordinated spine shrinkage, increased motility and turnover, and synaptic depression, without leading to synapse elimination, collectively designated here as “destabilization”, are not well understood7.

Epac2 (exchange protein directly activated by cAMP; cAMP-GEFII; RapGEF4) is a signaling protein previously detected in forebrain postsynaptic densities (PSD)8,9. However, its signaling functions in central spiny synapses are not well understood. Epac2 is a GEF for Rap, a Ras-like small GTPase which in its active form, promotes formation of thin spines and AMPAR endocytosis10–12, and is required for LTD, depotentiation10,13, LTP, and spatial memory storage14. Two genes, with complementary tissue distributions, encode Epac proteins: Epac2 is highly enriched in the brain and adrenal glands, while Epac1 is expressed in most non-neural tissues and is far less abundant in the adult brain15. In addition to other domains, Epac2 contains a Rap-GEF domain, and two cAMP-binding domains, only one of which seems functional (Fig. 1a). Binding of cAMP enhances Epac’s GEF activity toward Rap16. *In vitro* and in non-neuronal cells, both Epac1 and 2 activate Rap1 and 216. Epac proteins therefore represent a novel class of PKA-independent cAMP targets15,16, linking cAMP signaling to regulation of small GTPase function in neurons. A screen for candidate genes within the 2q21–33 autism susceptibility region identified rare nonsynonymous variants in the *EPAC2* gene17. These missense mutations segregated with autistic family members and were not present in a large number of unafflicted control individuals. However, it is unknown whether these mutations affect protein function or neuronal phenotypes.

Neuroligins (NLs) are postsynaptic adhesion molecules which bind to presynaptic neurexins. NLGN3 and NLGN4, as well as neurexin1 (NRXN1), have been genetically associated with autism18. NLs regulate synapse morphology19 and the balance between excitatory and inhibitory synapses20,21. However, little is known about the postsynaptic signaling by NLs.

Here we examined the functions and regulation of Epac2 in spines. Our data support a role for Epac2 in promoting synapse structural destabilization, associated with spine shrinkage, enhanced turnover, but without synapse elimination, paralleled by functional depression due

to removal of GluR2/3-containing AMPAR. Furthermore, two disease-associated Epac2 mutations alter protein function, synaptic protein distribution, and spine morphology, suggesting potential contributions to disease states.

RESULTS

Epac2 participates in postsynaptic protein complexes

While several studies reported a significant enrichment of Epac2 over Epac1 in brain15,22, some uncertainty still persists over this issue. To compare the abundance of Epac2 *vs.* Epac1 in cortical pyramidal neurons with largely stable synapses approaching maturity (div 28), we performed qPCR analysis of mRNA. Epac2 mRNA was enriched 32-fold over Epac1 mRNA in these neurons (Fig. 1b).

Proteomic studies detected Epac2 in forebrain postsynaptic densities8,9. To investigate its synaptic localization we immunostained cultured cortical neurons with an antibody that detects a single protein band of ~110 kDa in rat cerebral cortex (Fig. 1c). In pyramidal neurons (div 28) we detected Epac2 in punctate structures along dendrites (Fig. 1d), and in the soma, suggesting a functional role in dendrites. Epac2 colocalized with the synaptic markers bassoon, GluR2/3, PSD-95, and NR1, indicating enrichment in excitatory synapses (Fig. 1d–e). Colocalization of Epac2, PSD-95, NR1, and GluR2/3 signals in dendrites is quantified in Supplementary Fig. 1a–b. Together with Supplementary Fig. 2a–e, these data show that a significant amount of Epac2 is present in synapses and spines, in addition to other subcellular compartments. Small puncta of Epac2 signal were also detected in axons and colocalized with tau (Supplementary Fig. 2g). Epac2 may thus participate in protein complexes with postsynaptic proteins. Epac2 coimmunoprecipitated with the postsynaptic density (PSD) scaffolding protein PSD-95 from rat forebrain homogenates (Supplementary Fig. 1d), indicating that they participate in the same postsynaptic protein complexes.

Specific pharmacological activation of Epac2 in neurons

Epac2 is one of the two known PKA-independent cAMP targets: binding of cAMP to its C-terminal cAMP-binding domain enhances its GEF activity *in vitro* and in non-neuronal cells16. The cAMP analog 8–(4-chloro-phenylthio)-2'-O-methyladenosine-3',5'-cyclic monophosphate (8-CPT) specifically activates Epac, but not PKA16, and has been extensively used to study Epac function (Supplementary discussion and Supplementary Fig. 3a–c). The 8-CPT concentrations used in this study were similar to those used in other cell types and to the concentration required for half-maximal activation of Epac216,23,24. Incubation of cultured cortical neurons with 8-CPT induced Rap activation (Fig. 1f, *P<0.001). Since mature cortical neurons express small amounts of Epac1 relative to Epac2 (Fig. 1b)15, effects of 8-CPT on these neurons are mainly due to Epac2 activation. Incubation with 8-CPT did not cause CREB phosphorylation (Fig. 1g), a known PKA-dependent target of cAMP16, whereas treatment with BDNF, a known activator of CREB, phosphorylated CREB. Incubation with 8-CPT enhanced Epac2 dendritic clustering (Supplementary Fig. 3d). 8-CPT may also activate Rap1 signaling by the direct phosphorylation of Rap1 by PKA, or through C3G or PDZ-GEF125.

Epac2 activates Rap and causes spine shrinkage

To determine whether Epac2 activation stimulated Rap signaling in dendrites *in situ*, we examined the effect of 8-CPT on the phosphorylation of a known Rap target, B-Raf25,26. 8-CPT incubation significantly increased dendritic phospho-B-Raf (Fig. 1h–j, *P<0.001). This effect was not Ras-dependent, as it was not blocked by the Ras inhibitor FTase II (Supplementary Fig. 4). To determine the dependence on Epac2, we used RNA interference (RNAi) to knock down endogenous Epac2. The specificity of the RNAi for Epac2 was tested in hEK293 cells and in neurons (Supplementary Fig. 5 and 6). Epac2 knockdown prevented B-Raf phosphorylation (Fig. 1i–j), demonstrating Epac2-dependence and specificity.

To determine whether activation of endogenous Epac2 caused structural modifications in spines, we incubated mature GFP-expressing cultured pyramidal neurons (div 28) with 8-CPT (50 μM, 1 hr). This treatment induced shrinkage of existing spines exhibited by a reduction in average spine area, breadth and breadth/length ratios, without affecting spine linear density (Supplementary Fig. 7b). Incubation with 8-CPT for 24 hrs did not affect spine density.

To determine the requirement for Epac2 for basal and 8-CPT-induced spine morphology, we knocked down endogenous Epac2. Neurons were transfected with Epac2-specific shRNA that coexpressed GFP; in RNAi-expressing neurons, 8-CPT was incapable of inducing spine shrinkage, demonstrating that normal levels of Epac2 expression were required for 8-CPT-dependent spine shrinkage (Fig. 2a–b). Epac2 knockdown caused increased basal average spine area. This effect was rescued by overexpression of a “rescue Epac2” mutant, in which 3 silent point mutations have been introduced to render it RNAi-insensitive, demonstrating the specificity of the knockdown (Fig. 2a–b). RNAi knockdown of Epac2 did not affect spine density (Supplementary Fig. 6d–e).

The effects of Epac2 activation on spine morphology were specifically dependent on Epac2 Rap-GEF activity because in neurons overexpressing Epac2 lacking the catalytic portion of the Rap-GEF domain (Epac2-ΔGEF), 8-CPT did not induce spine shrinkage (Fig. 2c–d). These neurons had significantly larger spines than those overexpressing wild-type Epac2 (*P<0.001). The effects of Epac2 activation were occluded by overexpression of dominant-negative Rap1 and Rap2 (Rap1-DN and Rap2-DN) (Supplementary Fig. 7c). As expected, Epac2 overexpression did not alter spine area (Supplementary Fig. 6f–g), since the default state of Epac2 is autoinhibitory and it requires activation in order to activate Rap16.

To determine if 8-CPT affected the morphology of presynaptic terminals, we visualized presynaptic active zones with an antibody against bassoon. Epac2 activation significantly reduced the extent of presynaptic overlap with spines as revealed by quantification of the intensities of bassoon immunofluorescence overlapping with individual spines (Supplementary Fig. 7f) (*P<0.001), suggesting the possibility of reduced pre-postsynaptic apposition and weaker synapses. These effects on spine/bassoon overlap were occluded by Epac2 RNAi (Supplementary Fig. 7f). Incubation with 8-CPT also caused a reduction in bassoon immunoreactive cluster size (Supplementary Fig. 7e), indicating a potential presynaptic effect. These data provide evidence that Epac2 activation induces shrinkage of

spines and reduction of presynaptic contacts, and that these effects require Epac2's Rap-GEF activity.

Epac2 activation enhances spine motility

In vivo studies have revealed that smaller and thinner spines, morphologically resembling those induced by Epac2 activation, are very dynamic and undergo rapid remodeling, while large spines are stable1. To test whether Epac2 activation affected spine motility and turnover, we performed time-lapse imaging of GFP-expressing cortical neurons (Fig. 2e–g). As indicated by color-coded and overlaid images taken at three equally-separated time points during the imaging session, spines in control neurons were largely unchanged over the imaging period (80 min), undergoing only limited remodeling ("morphing"). On the contrary, extensive spine morphing, motility, and turnover were detectable in 8-CPT-treated neurons (Fig. 2e): Spines retracted, formed, or were transient (Supplementary Fig. 8b). Quantification of total spine motility demonstrated a ~62% increase in motility upon Epac2 activation (Fig. 2f) (*P<0.001). 8-CPT did not increase spine motility in Epac2-RNAi-expressing neurons, demonstrating that Epac2 is required for 8-CPT-dependent increased spine motility (Supplementary Fig. 8c–e). Time-lapse imaging of the same spine before and after 8-CPT perfusion further confirmed Epac2-dependent spine shrinkage (Fig. 2g–h) (*P<0.01). These data indicate that Epac2 activation causes structural destabilization of spines resulting in overall increased motility.

Epac2 activation promotes AMPAR removal from spines

As spine morphology, stability and function are coordinated2, Epac2 may also regulate glutamate receptor function in synapses. In cortical neurons, Epac2 coimmunoprecipitated with GluR2/3 AMPAR subunits, but not with GluR1 (Fig. 3a). Significant colocalization between Epac2 and GluR2/3 was observed in spines and dendrites (Fig. 1d, quantified in Supplementary Fig. 1b). This interaction places Epac2 in proximity to a subset of AMPARs, potentially allowing for their rapid regulation. To determine whether GluR2/3 content in spines was altered by Epac2 activation, we measured the integrated intensities of GluR2/3 immunofluorescence signals in individual spines (Fig. 3b–c). Following 8-CPT treatment, GluR2/3 content became significantly reduced in spines (Fig. 3b), and increased in shaft clusters. These effects were specifically dependent on Epac2; RNAi-mediated knockdown prevented 8-CPT-induced GluR2/3 removal from spines (Fig. 3c) (*P<0.01). RNAi expression did not alter GluR2/3 spine content, suggesting that Epac2 activation is only involved in GluR2/3 removal from synapses. GluR1 or NR1 cluster intensities were not affected by 8-CPT (Fig. 3d). Incubation with 8-CPT also resulted in a significant reduction in GluR2/3-bassoon overlap (Fig. 3e) (*P<0.05), along with a trend towards reduced GluR2/3-bassoon colocalized puncta number (Supplementary Fig. 7g). Thus, in addition to destabilizing spines, Epac2 activation also removes GluR2/3-containing AMPARs from synapses, potentially leading to weaker synaptic connections.

Epac2 activation depresses excitatory transmission

To determine the functional outcome of this reduction in GluR2/3 content in spines, we examined the effects of 8-CPT on AMPAR-dependent miniature excitatory postsynaptic

currents (mEPSCs) (Fig. 4). Incubation of neurons with 8-CPT (50 μM, 1 hr) resulted in a robust reduction of mean amplitudes (34%) and frequencies (59%) of AMPAR-mediated mEPSCs (Fig. 4a) (*P<0.05), resulting in a shift in the distribution of mEPSC amplitudes toward smaller values. RNAi-knockdown of Epac2 in postsynaptic neurons prevented 8-CPT-mediated reduction in basal mean mEPSC amplitude (Fig. 4a), confirming the Epac2-specificity of the 8-CPT effect. RNAi expression did not increase AMPAR mEPSCs, consistent with our immunostaining data. Interestingly, presence of RNAi in the postsynaptic cell did not affect the 8-CPT-dependent reduction in mEPSC frequencies (*P<0.01), suggesting that these effects were caused by activation of presynaptic Epac2, dissociating the pre- and postsynaptic actions of Epac2.

Perfusion of neurons with 8-CPT also resulted in rapid (~10 min), significant reduction of mean amplitudes of AMPAR mEPSCs (Fig. 4b) (*P<0.05), without significantly affecting mean frequencies. For all manipulations, the rise and decay time of mEPSCs were not affected. These results demonstrate that postsynaptic Epac2 activation rapidly and robustly depresses AMPAR-mediated synaptic transmission by reducing GluR2/3-containing AMPAR content in spines. Activation of Epac2 also caused a reduction in mEPSC frequencies, suggesting potential presynaptic effects.

Epac2 mediates dopamine-dependent synaptic remodeling

We next examined the upstream mechanisms regulating Epac2 in cortical pyramidal neurons. Epac2 is one of the few PKA-independent targets of cAMP. In neurons, cAMP levels are elevated by dopamine activation of the D1/D5 G-protein coupled receptor (DAR-D1/D5); in non-neuronal cells D1/D5 activation enhances Epac activity. Therefore, we tested whether Rap1 activity in neurons was enhanced by activation of DAR-D1/D5. Incubation of neurons with the D1/D5-specific agonist SKF-38393 (20 μM, 30 min) induced an enhancement of Rap1 activity comparable with that caused by 8-CPT (Fig. 5a) (*P<0.05). To determine if DAR-D1/D5 activation stimulated Rap1 activity in dendrites, we examined the effect of SKF-38393 on B-Raf phosphorylation (Fig. 5b). Incubation of neurons with SKF-38393 significantly increased B-Raf phosphorylation *in situ* in dendrites.

DAR-D1/D5 signaling has not yet been investigated in regards to spine plasticity. Incubation of neurons with SKF-38393 (20 μM, 30 min) caused a reduction in spine areas (Fig. 5c–d) (*P<0.001). In the presence of Epac2 RNAi, the effect of SKF-38393 on dendritic spines was occluded (Fig. 5c–d); treatment with SKF-38393 did not affect linear density (Supplementary Fig. 6e). Furthermore, SKF-38393 caused a significant reduction in surface GluR2 on spines (Fig. 5c, e) (*P<0.001). This effect required Epac2, as it did not occur when Epac2 was knocked down. Together, these data indicate that DAR-D1/D5 activation induces Rap1 activation, as well as Epac2-dependent spine shrinkage and GluR2 removal from spines.

Epac2 complexes with neuroligins

NLs are a class of synaptic adhesion molecules that modulate synapse morphology and excitatory/inhibitory synapse balance20. NL3 and 4 have also been genetically associated with autism27. We reasoned that Epac2 may participate in protein complexes with NLs. By

coimmunoprecipitation from cortical neurons, we found that NL3 and 1 strongly and specifically interacted with Epac2 (Fig. 6a). Epac2 also interacted with NL2, albeit more weakly than with NL3 or 1. Epac2 did not interact with N-cadherin, another synaptic adhesion molecule. Reverse coimmunoprecipitation confirmed the interaction of Epac2 with NL1 and 3 (Fig. 6b). Epac2 immunoprecipitated NL1 and 3, and to a lesser extent NL2, from rat cortex (Fig. 6c). This interaction was enhanced by 8-CPT (Supplementary Fig. 9a). HA-Epac2 immunoprecipitated NL3 or PSD-95 when these proteins were overexpressed in hEK293 cells, suggesting that they are members of a complex (Supplementary Fig. 9b). Consistent with this, Epac2 colocalized with NL1 and 3 in a large fraction of spine-like structures (Fig. 6d, Supplementary Fig. 1c). We hypothesized that NLs could potentially recruit Epac2 to the plasma membrane. To test this we used COS7 cells; GFP-Epac2 expressed alone was diffusely distributed in the cytosol, while HA-NL3 expressed alone was at the plasma membrane (Fig. 6e). In contrast, when coexpressed with NL3, a fraction of Epac2 was recruited to the plasma membrane (Fig. 6e). Similarly, overexpression of NL3 enhanced Epac2 localization to the membrane in dendrites (Supplementary Fig. 9c, d).

We next sought to determine whether Epac2 activation altered Epac2 colocalization with NL3 in neurons. Neurons treated with 8-CPT exhibited more Epac2/NL3 colocalized puncta (Fig. 6f), an effect driven by increased Epac2 immunoreactive puncta (Supplementary Fig. 3d); NL3 puncta were not affected (Fig. 6f, Supplementary Fig. 9e). As Epac2 translocation to the plasma membrane is associated with its activation28, we reasoned that NL3 may activate Epac2. Indeed, coexpression of Epac2 with NL3 robustly enhanced its Rap-GEF activity (Fig. 6g–h) (*P<0.001). Collectively these data suggest that Epac2 and NL1/3 form protein complexes in neurons, that NL3 is capable of recruiting Epac2 to the plasma-membrane, that Epac2 proximity to NL3 is modulated in parallel with Epac2 activation, and that NL3 enhances Epac2 Rap-GEF activity.

Disease-associated mutants of Epac2 affect Rap signaling

Four rare coding mutations in Epac2 (M165T, V646F, G706R, and T809S) have been genetically associated with autism17 (“*” in Supplementary Fig. 10a). These rare variants strictly segregated with autistic family members, and were not present in unafflicted individuals. To test whether these mutations affected protein function and synapse morphology, we generated point mutants of the Epac2 protein that corresponded to these variants (Supplementary Fig. 10a–b). We first examined if Epac2 mutations affected Rap-GEF activity, by measuring Rap1-GTP in hEK293 cells transfected with Epac2 or its mutants. The Epac2-V646F mutation impaired the Rap-GEF activity of Epac2 (Fig. 7a–b) (*P=0.01). As NL3 enhanced Epac2 activity, we examined the effects of Epac2’s disease-associated mutations on NL3-dependent stimulation of its GEF activity (Fig. 7c–d). Coexpression of NL3 with Epac2-V646F resulted in reduced Rap activation, similar to the effect of this mutation on basal Rap-GEF activity. Conversely, coexpression of NL3 with Epac2-T809S increased its Rap-GEF activity (*P<0.001). We next examined the effects of Epac2 mutations on dendritic B-Raf phosphorylation (Fig. 7e–f). Consistent with the above data, expression of Epac2-V646F reduced dendritic phospho-B-Raf immunofluorescence, indicative of reduced Rap signaling in dendrites. Conversely, Epac2-T809S increased

dendritic phospho-B-Raf immunofluorescence, indicative of increased Rap signaling in dendrites (*P<0.001). The M165T and G706R mutations did not affect Epac2 function.

Disease-associated mutants of Epac2 alter spine morphology

As they affected protein function, we hypothesized that some of Epac2 mutations may affect spine morphology. Overexpression of two of the mutants in neurons (div 28) affected spine morphology (Fig. 8a–b). Epac2-V646F caused a significant increase in average spine area (*P<0.001) (Fig. 8b). Epac2-T809S increased spine average linear density (*P<0.001). To gain insight into the potential mechanisms underlying the spine morphological changes, we examined the effects of Epac2 mutations on the average intensity and number of PSD-95 immunofluorescent puncta in dendrites (Fig. 8c–d). Overexpression of PSD-95 has been previously shown to induce synaptogenesis and increased spine number7. Expression of Epac2-V646F increased PSD-95 immunofluorescence average intensity in individual puncta, consistent with its effect on spine size (*P<0.001). Conversely, Epac2-T809S increased the number of PSD-95 clusters along dendrites, consistent with its effect on spine density (*P<0.001). These data indicate that the Epac2-V646F and Epac2-T809S variants affect protein function and dendritic spine morphology.

DISCUSSION

Taken together, our studies identify a novel mechanism that promotes the dynamic remodeling of spiny synapses on cortical pyramidal neurons, actively destabilizing spines by promoting their shrinkage and increasing their motility, in parallel with removing GluR2/3-containing AMPAR and depressing glutamatergic transmission (Supplementary Fig. 11). Similar effects are caused by the stimulation of DAR-D1/D5s; these effects are prevented by postsynaptic knockdown of Epac2. Interestingly, two disease-associated Epac2 mutations affect protein function and dendritic Rap signaling, and their expression in pyramidal neurons affects spine morphology and PSD-95 clustering. Because synapse dynamic remodeling is important in the maturation, refinement, and plasticity of brain circuits, and may malfunction in some disorders, our studies implicate Epac2 as having a role in normal and pathological brain plasticity.

Epac2 activation enhances spine dynamic remodeling, consisting of spine shrinkage, turnover, head morphing, and reduced overlap with presynaptic release sites (Supplementary Fig. 11). Conversely, Epac2 inactivation causes spine enlargement and stabilization. However, Epac2 does not promote synapse elimination. Spine shrinkage occurs during various forms of brain plasticity, including hippocampal LTD3,4. Small, thin, and highly dynamic spines play an important role in the development, refinement, and experience-dependent plasticity of cortical neuronal circuits1,5. While filopodia in young neurons are highly motile, spines with mature morphologies are more stable. However, even in the mature cortex, there is a steady state of spine morphing and turnover, modulated by physiological stimuli, such as experience1,2. Epac2 may thus promote the dynamic remodeling of such otherwise stable spines. Few molecules, upon activation, are known to promote spine shrinkage and increased motility without elimination7 (Supplemental Text).

Epac2 activation caused a reduction in AMPAR content in spines along with reduced amplitude and frequency of AMPAR-mediated mEPSCs, indicating Epac2 also depresses glutamatergic transmission. Epac2 specifically regulates GluR2/3, likely due to the participation of Epac2, along with PSD-95, in protein complexes with GluR2/3. In these complexes, Epac2 can respond to stimuli and activate Rap, which in turn diffuses to nearby GluR2/3 receptors and triggers their internalization. Our data suggest that Epac2 activation selectively removes GluR2/3 subunit-containing AMPARs from synapses; the remaining synaptic AMPARs may thus consist of a larger fraction of GluR1/GluR2-containing receptors, and fewer GluR2/GluR3-containing receptors. As GluR2/3 is removed from spines, the total amount of functional AMPARs is reduced, leading to reduced AMPAR mEPSC amplitudes.

Epac2-dependent changes in synaptic GluR2/3 content may contribute to several types of plasticity29,30. A range of effects of 8-CPT incubation have been reported in different neuronal preparations. Short-term and transient presynaptic potentiation has been reported in invertebrate neuromuscular junctions31,32, the calyx of Held, and in young hippocampal and cortical neurons33 (Supplemental Text). Postsynaptically, based on 8-CPT responsiveness, recent studies found PACAP-, protein synthesis- and ERK-dependent LTD34, and facilitation of βAR-, HFS-, protein synthesis-, and ERK-dependent LTP, without affecting LTP induction35. One potential explanation for these diverging effects is that transient destabilization could make synapses more receptive to subsequent activity-dependent potentiating or depressing stimuli, leading to LTP or LTD, respectively12. Modulation of synapses by Epac proteins may also affect cognitive functions and behavior. Epac and PKA are jointly required for hippocampal memory retrieval36, and Epac activation with 8-CPT rescued psychiatric disease-related deficits in sensory motor gating and memory, caused by overactivation of $G\alpha_s$ signaling37.

cAMP signaling is important in synaptic plasticity, learning, memory38, psychiatric disease, and drug addiction. Most previous work on cAMP signaling in pyramidal neurons focused on its actions through PKA. However, several studies report that postsynaptic cAMP-dependent but PKA-independent mechanisms induce LTD, depress basal synaptic transmission, and reverse potentiation39. In dendrites, cAMP is produced upon activation of G_s-coupled receptors, such as D1-like receptors. Little is known about the mechanisms of regulation of spine morphology by dopamine signaling. We show that DAR-D1/D5 activation stimulates dendritic Rap signaling, causing Epac2-dependent spine shrinkage and GluR2 removal. In cortical pyramidal neurons, DAR-D1/D5s control plasticity bidirectionally, inducing both LTD and LTP40,41. Dopamine also facilitates LTD in rat prefrontal cortex42, and application of cAMP under specific conditions depresses synaptic transmission38,43. Epac activation rescued $G\alpha_s$ signaling overactivation-induced deficits in animals37. Other studies reported dopamine- and D1-dependent enhancement of synaptic transmission44. The specific conditions under which dopamine signaling promotes potentiation or depression are incompletely understood. Our data indicate that Epac2 mediates neuromodulation by DAR-D1/D5, and link dopamine signaling with synapse structural remodeling.

Epac2 participates in protein complexes with NL1 and 3, and these proteins show extensive colocalization in dendrites. Our data suggest that NL3 recruits Epac2 to the plasma membrane, and enhances its Rap-GEF activity. Enhanced Epac2 activity promotes spine shrinkage and increased spine dynamics. NLs are synaptic adhesion molecules previously shown to promote synapse formation and maturation19,20,21. Such seemingly opposite functions are also simultaneously performed by another class of synaptic adhesion molecules, ephrinB/EphB, which promote filopodia motility and motility-dependent synaptogenesis45. As suggested for EphB45, NL/Epac2/Rap signaling may promote local sampling of the presynaptic environment through increased spine motility, also providing trans-cellular interaction between the dynamic spines and newly contacted presynaptic terminals.

NLs and their ligands neurexins are associated with autism spectrum disorders (ASD). Chromosomal regions of *NLGN3*, *NLGN4*, and *NRXN1* have been implicated in ASD27,46, but rare mutations in these genes do not account for the strong association of their loci with ASD. Mutations in *NLGN3* and *NLGN4* detected in autistic individuals encode proteins with altered function46. Interaction with NLs places Epac2 in functional proximity to proteins that have previously been implicated in ASD, suggesting participation in the same synaptic signaling network.

A screen in autistic individuals identified four rare non-synonymous variants in the *EPAC2* gene17. We found that two of these mutations affected protein function, signaling, and synapse remodeling. Specifically, Epac2-V646F impaired the basal GEF activity, Rap-dependent signaling in dendrites, leading to larger spines, and larger PSD-95 clusters (Supplementary Fig. 11c). These effects are similar to those caused by Epac2 knockdown or Epac2-ΔGEF, and can be explained by reduced GEF activity. On the other hand, the Epac2-T809S was more responsive to NL3-dependent enhancement of its GEF activity, leading to increased Rap signaling in dendrites (Supplementary Fig. 11d). Its neuronal expression increases spine density, likely due to an increased responsiveness to NL3-dependent enhancement of its GEF activity and to increased clustering of PSD-95, a molecule with established synaptogenic properties. While the other two mutations did not affect any of the tested parameters, this does not exclude potential effects on other neuronal properties, or interaction with other unknown genetic or environmental factors. Aberrant synaptic connectivity is thought to occur in autism and comorbid diseases including fragile-X, and increased cortical dendritic spine density has been reported in some individuals with autism6. Understanding Epac2 function in spines may therefore shed light on normal and disease-associated spine plasticity.

Supplementary Material

Refer to Web version on PubMed Central for supplementary material.

Acknowledgements

We thank Dr. Richard L. Huganir (Johns Hopkins University) for AMPAR and NMDAR subunit antibodies; Dr. Johannes Bos (Utrecht University) and Dr. Phillip Stork (Vollum Institute) for plasmids; Dr. Alaa El-Husseini (University of British Columbia) and Dr. Peter Scheiffele (University of Basel) for neuroligin antibodies and

plasmid constructs, Dr. Gary Borisy and Dr. Shin-ichiro Kojima (Northwestern University) for the pGSuper plasmid. We thank Dr. Anand K. Srivastava (J.C. Self Research Institute of Human Genetics, Greenwood Genetic Center) and Dr. Geoffrey Swanson (Northwestern University) for thoughtful discussion. This work was supported by the National Alliance for Autism Research (NAAR), the National Alliance for Research on Schizophrenia and Depression (NARSAD), Alzheimer's Association, NIH grant MH 071316 to P.P., NIH grant (NS057499) to M. P., NIH grant CA108647 to L.A.Q, a pre-doctoral American Heart Association (AHA) fellowship to K.M.W., and a post-doctoral AHA fellowship to D.P.S.

REFERENCES

1. Holtmaat AJ, et al. Transient and persistent dendritic spines in the neocortex in vivo. Neuron. 2005; 45:279–291. [PubMed: 15664179]
2. Kasai H, Matsuzaki M, Noguchi J, Yasumatsu N, Nakahara H. Structure-stability-function relationships of dendritic spines. Trends Neurosci. 2003; 26:360–368. [PubMed: 12850432]
3. Nagerl UV, Eberhorn N, Cambridge SB, Bonhoeffer T. Bidirectional activity-dependent morphological plasticity in hippocampal neurons. Neuron. 2004; 44:759–767. [PubMed: 15572108]
4. Zhou Q, Homma KJ, Poo MM. Shrinkage of dendritic spines associated with long-term depression of hippocampal synapses. Neuron. 2004; 44:749–757. [PubMed: 15572107]
5. Oray S, Majewska A, Sur M. Dendritic spine dynamics are regulated by monocular deprivation and extracellular matrix degradation. Neuron. 2004; 44:1021–1030. [PubMed: 15603744]
6. Pickett J, London E. The neuropathology of autism: a review. J Neuropathol Exp Neurol. 2005; 64:925–935. [PubMed: 16254487]
7. Tada T, Sheng M. Molecular mechanisms of dendritic spine morphogenesis. Curr Opin Neurobiol. 2006; 16:95–101. [PubMed: 16361095]
8. Jordan BA, et al. Identification and verification of novel rodent postsynaptic density proteins. Mol Cell Proteomics. 2004; 3:857–871. [PubMed: 15169875]
9. Peng J, et al. Semiquantitative proteomic analysis of rat forebrain postsynaptic density fractions by mass spectrometry. J Biol Chem. 2004; 279:21003–21011. [PubMed: 15020595]
10. Zhu JJ, Qin Y, Zhao M, Van Aelst L, Malinow R. Ras and Rap control AMPA receptor trafficking during synaptic plasticity. Cell. 2002; 110:443–455. [PubMed: 12202034]
11. Xie Z, Huganir RL, Penzes P. Activity-dependent dendritic spine structural plasticity is regulated by small GTPase Rap1 and its target AF-6. Neuron. 2005; 48:605–618. [PubMed: 16301177]
12. Srivastava DP, et al. Rapid enhancement of two-step wiring plasticity by estrogen and NMDA receptor activity. Proc Natl Acad Sci U S A. 2008
13. Zhu Y, et al. Rap2-JNK removes synaptic AMPA receptors during depotentiation. Neuron. 2005; 46:905–916. [PubMed: 15953419]
14. Morozov A, et al. Rap1 couples cAMP signaling to a distinct pool of p42/44MAPK regulating excitability, synaptic plasticity, learning, and memory. Neuron. 2003; 39:309–325. [PubMed: 12873387]
15. Kawasaki H, et al. A family of cAMP-binding proteins that directly activate Rap1. Science. 1998; 282:2275–2279. [PubMed: 9856955]
16. Bos JL. Epac proteins: multi-purpose cAMP targets. Trends Biochem Sci. 2006; 31:680–686. [PubMed: 17084085]
17. Bacchelli E, et al. Screening of nine candidate genes for autism on chromosome 2q reveals rare nonsynonymous variants in the cAMP-GEFII gene. Mol Psychiatry. 2003; 8:916–924. [PubMed: 14593429]
18. Abrahams BS, Geschwind DH. Advances in autism genetics: on the threshold of a new neurobiology. Nat Rev Genet. 2008; 9:341–355. [PubMed: 18414403]
19. Chih B, Afridi SK, Clark L, Scheiffele P. Disorder-associated mutations lead to functional inactivation of neuroligins. Hum Mol Genet. 2004; 13:1471–1477. [PubMed: 15150161]
20. Chih B, Engelman H, Scheiffele P. Control of excitatory and inhibitory synapse formation by neuroligins. Science. 2005; 307:1324–1328. [PubMed: 15681343]
21. Craig AM, Kang Y. Neurexin-neuroligin signaling in synapse development. Curr Opin Neurobiol. 2007; 17:43–52. [PubMed: 17275284]

22. Ulucan C, et al. Developmental changes in gene expression of Epac and its upregulation in myocardial hypertrophy. Am J Physiol Heart Circ Physiol. 2007; 293:H1662–H1672. [PubMed: 17557924]
23. Enserink JM, et al. A novel Epac-specific cAMP analogue demonstrates independent regulation of Rap1 and ERK. Nat Cell Biol. 2002; 4:901–906. [PubMed: 12402047]
24. Kang G, et al. Epac-selective cAMP analog 8-pCPT-2'-O-Me-cAMP as a stimulus for Ca2+-induced Ca2+ release and exocytosis in pancreatic beta-cells. J Biol Chem. 2003; 278:8279–8285. [PubMed: 12496249]
25. York RD, et al. Rap1 mediates sustained MAP kinase activation induced by nerve growth factor. Nature. 1998; 392:622–626. [PubMed: 9560161]
26. Vossler MR, et al. cAMP activates MAP kinase and Elk-1 through a B-Raf- and Rap1-dependent pathway. Cell. 1997; 89:73–82. [PubMed: 9094716]
27. Jamain S, et al. Mutations of the X-linked genes encoding neuroligins NLGN3 and NLGN4 are associated with autism. Nat Genet. 2003; 34:27–29. [PubMed: 12669065]
28. Li Y, et al. The RAP1 guanine nucleotide exchange factor Epac2 couples cyclic AMP and Ras signals at the plasma membrane. J Biol Chem. 2006; 281:2506–2514. [PubMed: 16316996]
29. Luthi A, et al. Hippocampal LTD expression involves a pool of AMPARs regulated by the NSF-GluR2 interaction. Neuron. 1999; 24:389–399. [PubMed: 10571232]
30. Xia J, Chung HJ, Wihler C, Huganir RL, Linden DJ. Cerebellar long-term depression requires PKC-regulated interactions between GluR2/3 and PDZ domain-containing proteins. Neuron. 2000; 28:499–510. [PubMed: 11144359]
31. Cheung U, Atwood HL, Zucker RS. Presynaptic effectors contributing to cAMP-induced synaptic potentiation in Drosophila. J Neurobiol. 2006; 66:273–280. [PubMed: 16329127]
32. Zhong N, Zucker RS. cAMP acts on exchange protein activated by cAMP/cAMP-regulated guanine nucleotide exchange protein to regulate transmitter release at the crayfish neuromuscular junction. J Neurosci. 2005; 25:208–214. [PubMed: 15634783]
33. Gekel I, Neher E. Application of an Epac activator enhances neurotransmitter release at excitatory central synapses. J Neurosci. 2008; 28:7991–8002. [PubMed: 18685024]
34. Ster J, et al. Epac mediates PACAP-dependent long-term depression in the hippocampus. J Physiol. 2009; 587:101–113. [PubMed: 19001039]
35. Gelinas JN, et al. Activation of exchange protein activated by cyclic-AMP enhances long-lasting synaptic potentiation in the hippocampus. Learn Mem. 2008; 15:403–411. [PubMed: 18509114]
36. Ouyang M, Zhang L, Zhu JJ, Schwede F, Thomas SA. Epac signaling is required for hippocampus-dependent memory retrieval. Proc Natl Acad Sci U S A. 2008; 105:11993–11997. [PubMed: 18687890]
37. Kelly MP, et al. Developmental etiology for neuroanatomical and cognitive deficits in mice overexpressing Galphas, a G-protein subunit genetically linked to schizophrenia. Mol Psychiatry. 2009; 14:398–415. 347. [PubMed: 19030002]
38. Frey U, Huang YY, Kandel ER. Effects of cAMP simulate a late stage of LTP in hippocampal CA1 neurons. Science. 1993; 260:1661–1664. [PubMed: 8389057]
39. Otmakhov N, Lisman JE. Postsynaptic application of a cAMP analogue reverses long-term potentiation in hippocampal CA1 pyramidal neurons. J Neurophysiol. 2002; 87:3018–3032. [PubMed: 12037205]
40. Chen Z, et al. Roles of dopamine receptors in long-term depression: enhancement via D1 receptors and inhibition via D2 receptors. Receptors Channels. 1996; 4:1–8. [PubMed: 8723642]
41. Huang YY, Simpson E, Kellendonk C, Kandel ER. Genetic evidence for the bidirectional modulation of synaptic plasticity in the prefrontal cortex by D1 receptors. Proc Natl Acad Sci U S A. 2004; 101:3236–3241. [PubMed: 14981263]
42. Otani S, Blond O, Desce JM, Crepel F. Dopamine facilitates long-term depression of glutamatergic transmission in rat prefrontal cortex. Neuroscience. 1998; 85:669–676. [PubMed: 9639264]
43. Gereau, RWt; Conn, PJ. Potentiation of cAMP responses by metabotropic glutamate receptors depresses excitatory synaptic transmission by a kinase-independent mechanism. Neuron. 1994; 12:1121–1129. [PubMed: 8185947]

44. Smith WB, Starck SR, Roberts RW, Schuman EM. Dopaminergic stimulation of local protein synthesis enhances surface expression of GluR1 and synaptic transmission in hippocampal neurons. Neuron. 2005; 45:765–779. [PubMed: 15748851]

45. Kayser MS, Nolt MJ, Dalva MB. EphB receptors couple dendritic filopodia motility to synapse formation. Neuron. 2008; 59:56–69. [PubMed: 18614029]

46. Sudhof TC. Neuroligins and neurexins link synaptic function to cognitive disease. Nature. 2008; 455:903–911. [PubMed: 18923512]

47. Kojima S, Vignjevic D, Borisy GG. Improved silencing vector co-expressing GFP and small hairpin RNA. Biotechniques. 2004; 36:74–79. [PubMed: 14740488]

48. Dunaevsky A, Tashiro A, Majewska A, Mason C, Yuste R. Developmental regulation of spine motility in the mammalian central nervous system. Proc Natl Acad Sci U S A. 1999; 96:13438–13443. [PubMed: 10557339]

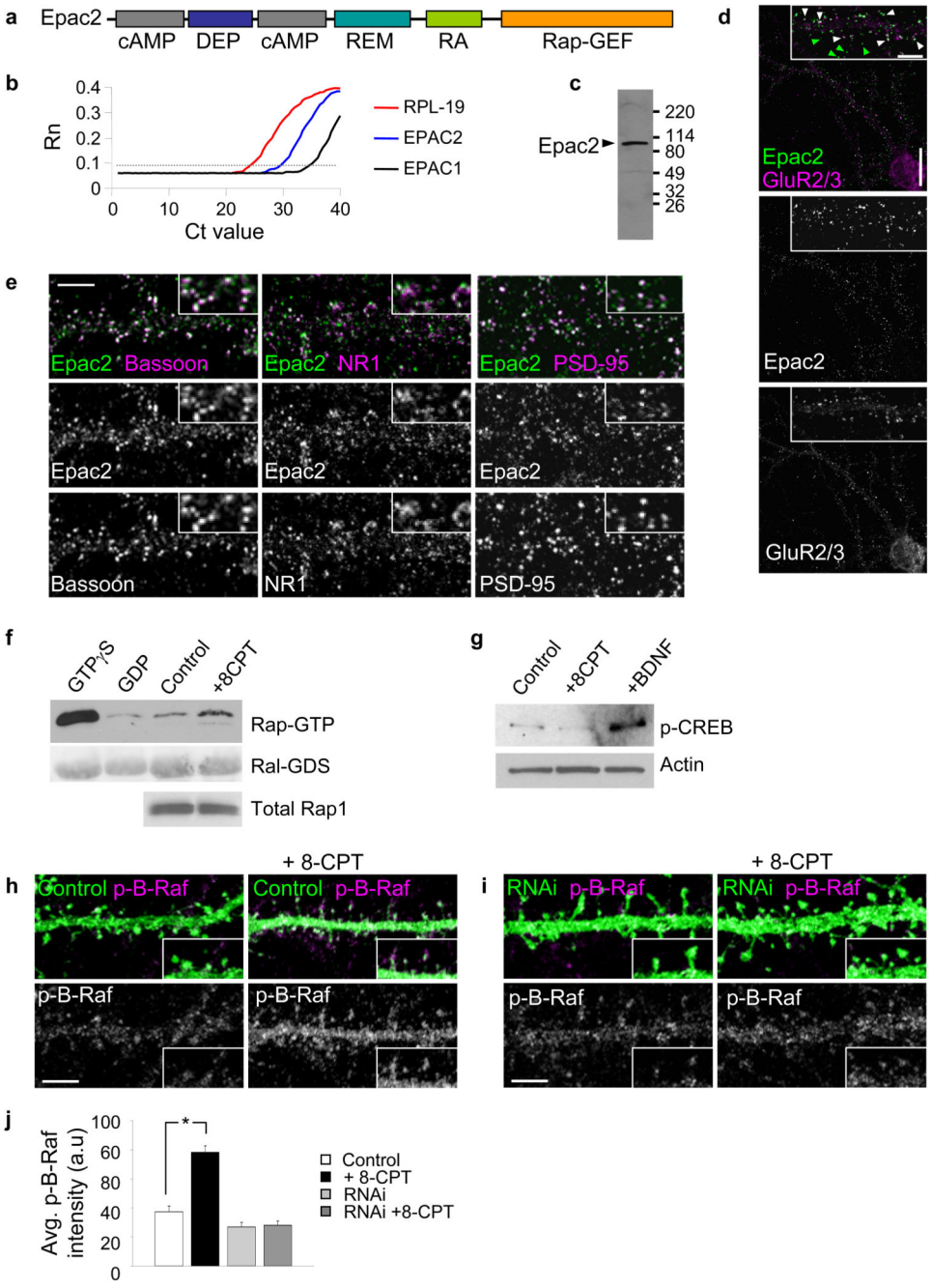

Figure 1.

Epac2 is present in synapses in cultured cortical pyramidal neurons. **(a)** Domain structure of Epac2. **(b)** Quantitative PCR analysis of Epac1 and Epac2 mRNA in cortical neurons (div 28) demonstrates the relative enrichment of Epac2. **(c)** Western blot detection of Epac2 in rat forebrain homogenate. **(d)** Localization of Epac2 in cultured cortical pyramidal neurons (div 28); colocalization with GluR2/3. White arrowheads, colocalization; green arrowheads, non-colocalized Epac2 puncta. **(e)** Double immunofluorescence with antibodies for synaptic proteins bassoon, NR1 and PSD-95. **(f)** Epac2 activation by 8-CPT (50 μM, 1 hr) in cortical

neurons; endogenous Rap activation was measured. Fold Rap activation compared to control: 1.57±0.11 fold increase, *P<0.001, *n* = 4. **(g)** Specificity of 8-CPT for Epac2 in neurons: effect of 8-CPT or BDNF on CREB phosphorylation, *n* = 3 **(h)** Effect of incubation with 8-CPT (50 μM, 1 hr) on the phosphorylation of the Rap target B-Raf *in situ* in pyramidal neuronal dendrites. **(i)** Effect of incubation with 8-CPT (50 μM, 1 hr) on B-Raf phosphorylation in dendrites of neurons expressing Epac2 RNAi. **(j)** Quantification of B-Raf fluorescence intensities in h-i (*P<0.001), *n* = 9–12 cells per condition, 3 experiments. Error bars: s.e.m. Scale bars: d, 15 μm; d-zoom, e, h, i, 5 μm.

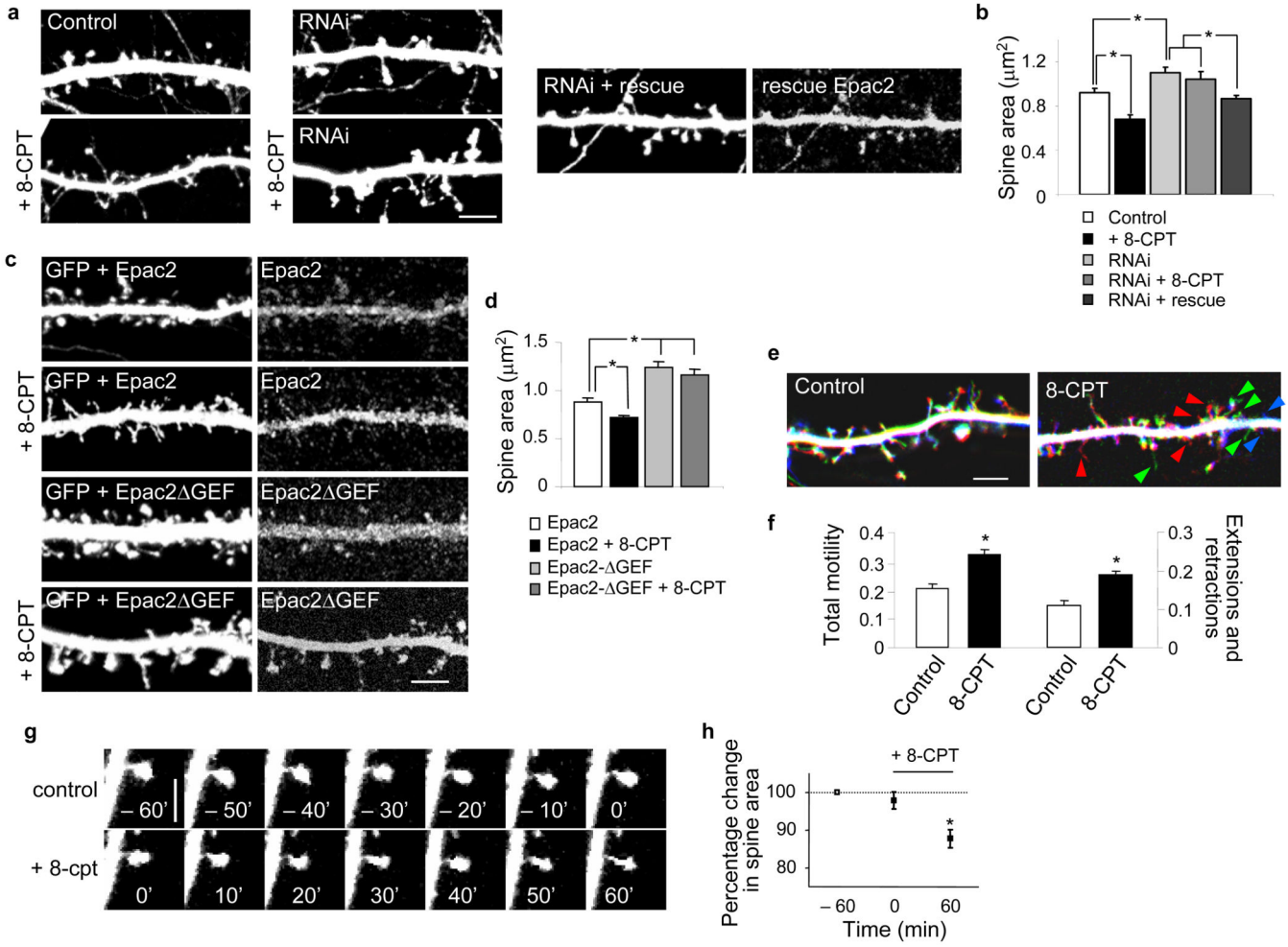

Figure 2.

Epac2 activation induces dendritic spine shrinkage, reduces presynaptic contact and enhances spine motility and turnover. **(a)** Effect of incubation with 8-CPT (50 μM, 1 hr), in absence or presence of Epac2 RNAi or rescue RNAi, on spine morphology. **(b)** Quantification of average spine areas in a; area (μm^2): control, 0.92±0.04; 8-CPT, 0.68±0.04; Epac2 RNAi, 1.10±0.05; Epac2 RNAi+8-CPT, 1.04±0.07; Epac2 RNAi+rescue, 0.87±0.03, *P<0.001. *n* = 102–252 spines, 5–10 cells per condition, 3 experiments (see also Supplementary Fig 7a,c). **(c)** Epac2 lacking the GEF domain (Epac2-ΔGEF) prevents 8-CPT-induced spine shrinkage. **(d)** Quantification of c; area (μm^2): Epac2, 0.88±0.05; Epac2+8-CPT, 0.72±0.03; Epac2ΔGEF, 1.24±0.06; Epac2 ΔGEF+8-CPT, 1.17±0.05, *P<0.001, *n* = 169–274 spines, 5–9 cells per condition, 3 experiments. All neurons were analyzed at div 28. **(e)** Time-lapse imaging of spine dynamics in GFP-expressing cortical pyramidal neurons (div 25) pretreated with or without 8-CPT (50 μM). Visualization of spine dynamics from the beginning, middle and end of 80-minute imaging sessions; red: retracting, green: transient, blue: newly extended. **(f)** Quantification of total spine motility, expressed as fraction of spines undergoing extension, retraction or head morphing, and fraction of spines undergoing extensions or retractions; normalized total motility: control, 0.21±0.02; 8-CPT, 0.34±0.01, *P<0.001, *n* = 1218 spines, 5 cells per condition. **(g)** Example

of time-lapse imaging of an individual spine before and after 8-CPT (50 μM, 1 hr) incubation; spine shrinks following 8-CPT treatment. **(h)** Quantification of g; -60 min, 100%; 0 min 97.9±3.0%; 60 min, 87.5±2.4%, *P<0.01, *n* = 84 spines, 3 experiments. Error bars: s.e.m. Scale bars: a, c, e 5μm; g, 2.5μm.

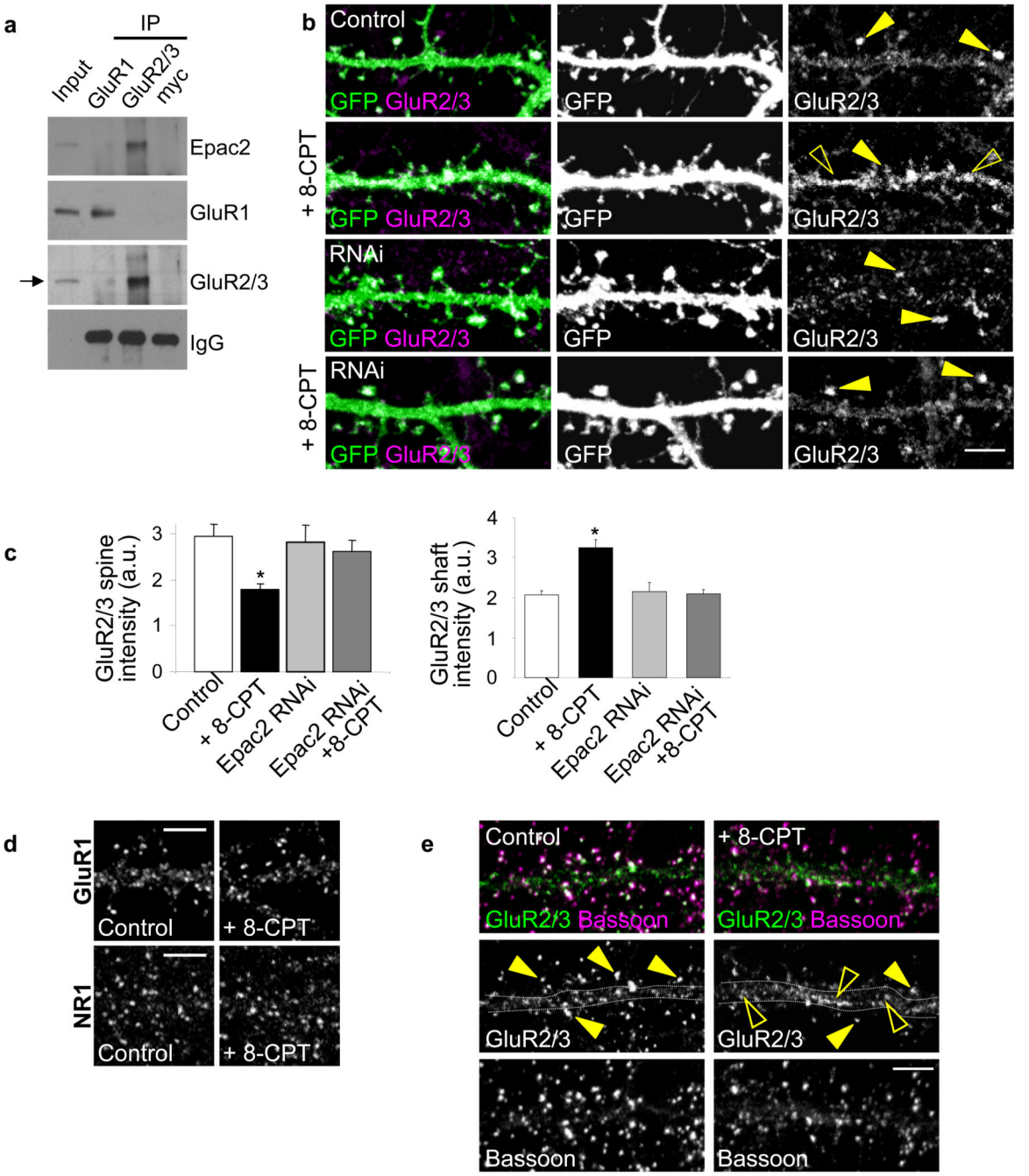

Figure 3.

Epac2 interacts with GluR2/3-containing AMPAR and removes them from spines. **(a)** Coimmunoprecipitation of Epac2 with GluR2/3 but not GluR1 from cortical neurons (div 28); myc, control antibody. **(b)** Effects of 8-CPT (50 μM, 1 hr) and Epac2 RNAi knockdown on GluR2/3 content in spine heads. GluR2/3 clusters were visualized in spines outlined by GFP (arrowhead, clusters in spines; open arrowhead, shafts) **(c)** Quantification of the effects in b on GluR2/3 signal intensity in spines (top) and shaft (bottom); GluR2/3 immunofluorescence (a.u.): control, 2.94±0.27; 8-CPT, 1.78±0.13; Epac2 RNAi, 2.81±.37;

Epac2 RNAi+8-CPT, 2.61±0.24,*P<0.01, *n* = 10–14 cells, 3 experiments. **(d)** GluR1 and NR1 cluster intensity was not affected: GluR1 immunofluorescence (a.u.): control, 1.29±0.12; 8-CPT, 1.08±0.11; NR1 immunofluorescence (a.u.): control, 0.95±0.04; 8-CPT, 1.05±0.08. *n* = 8–14 cells per condition. **(e)** Effect of 8-CPT on GluR2/3 colocalization with bassoon (arrowhead, clusters on spines; open arrowhead, shafts). Percent GluR2/3 puncta overlapping bassoon: control, 0.89± 0.02; 8-CPT, 0.80±0.03 (*P<0.05), *n* = 17 cells per condition. Error bars: s.e.m. Scale bars: 5μm. a.u.: arbitrary units.

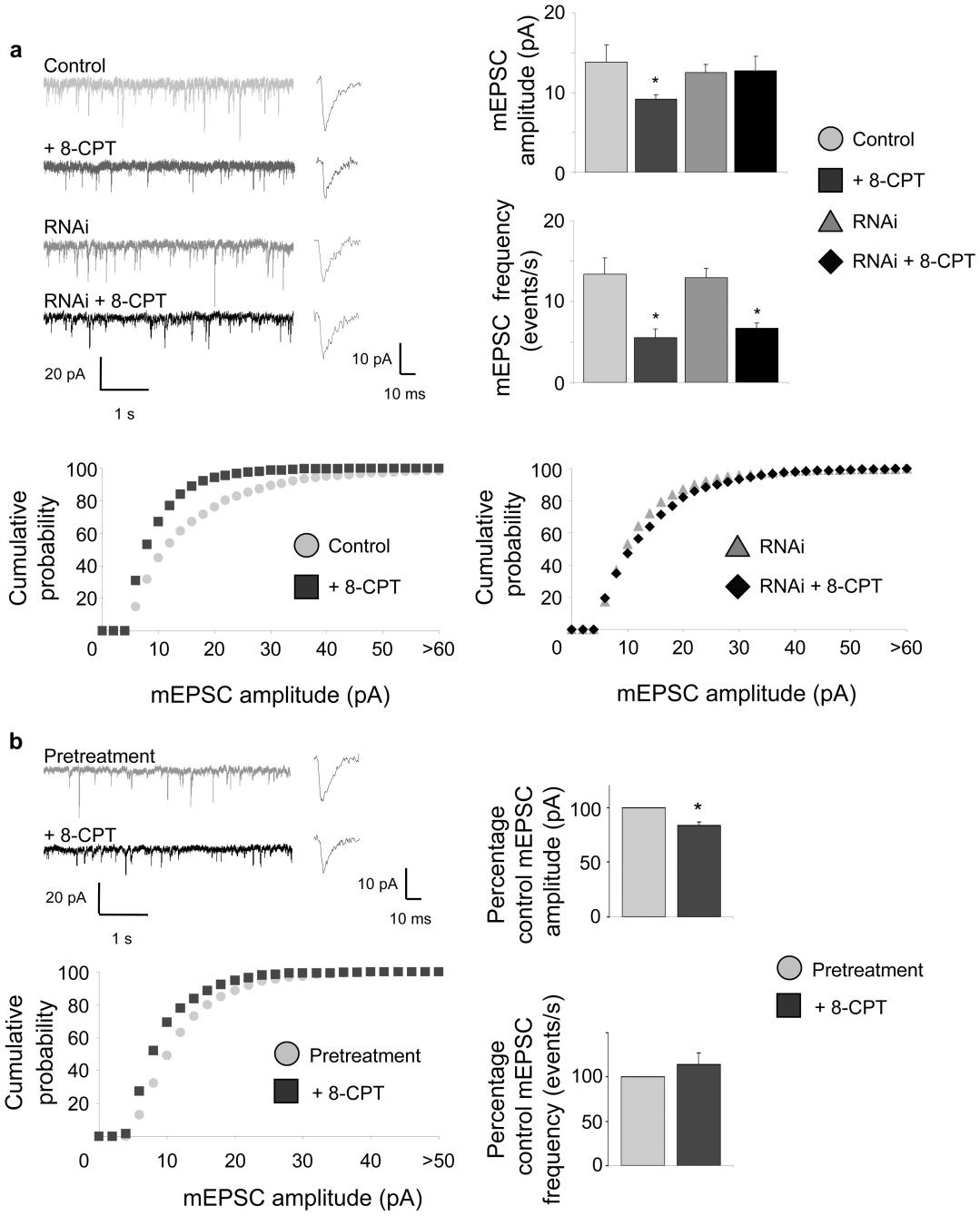

Figure 4.

Epac2 activation depresses AMPAR-mediated synaptic transmission. **(a)** Effect of 8-CPT on AMPAR-mediated mEPSC amplitudes and frequencies in pyramidal neurons (div 28). Synaptic currents were recorded in single cells pretreated with vehicle or 8-CPT (50 μM, 1 hr). Traces show representative recordings. Bar graphs: quantification of mean amplitudes (control (pA), 13.85±2.12; 8-CPT, 9.19±0.53, *P<0.05) and frequencies (control (events/s), 13.40±2.00; 8-CPT, 5.55±1.06, *P<0.01) of AMPAR-mediated mEPSCs. *n* = 9–11 cells per condition. Epac2 RNAi blocks 8-CPT-induced decrease in AMPAR-mediated mEPSC

amplitude (RNAi+vehicle (pA), 12.54±0.98; RNAi+8-CPT, 12.74±1.80), but not mEPSC frequency (RNAi+vehicle (events/s), 12.98±1.09; RNAi+8-CPT, 6.70±0.67,*P<0.01) $n = 5$ cells per condition. Cumulative probability plots show a shift of mEPSC amplitudes toward smaller values in response to 8-CPT treatment (left), while in Epac2 RNAi expressing cells, no difference in mEPSC amplitude distribution is detected (right). **(b)** Synaptic currents were recorded in single cells before (gray) and 10–15 min after (black) perfusion with 8-CPT (50 μM). This resulted in a rapid reduction of mean amplitude of AMPAR-mediated mEPSCs (post 8-CPT treatment, −16.51±3.65% relative to control mean pA, *P<0.05), but not frequency (post 8-CPT, +13.84±12.99% relative to control events/s). Insets: mEPSC rise and decay time. $n = 3$. Error bars: s.e.m.

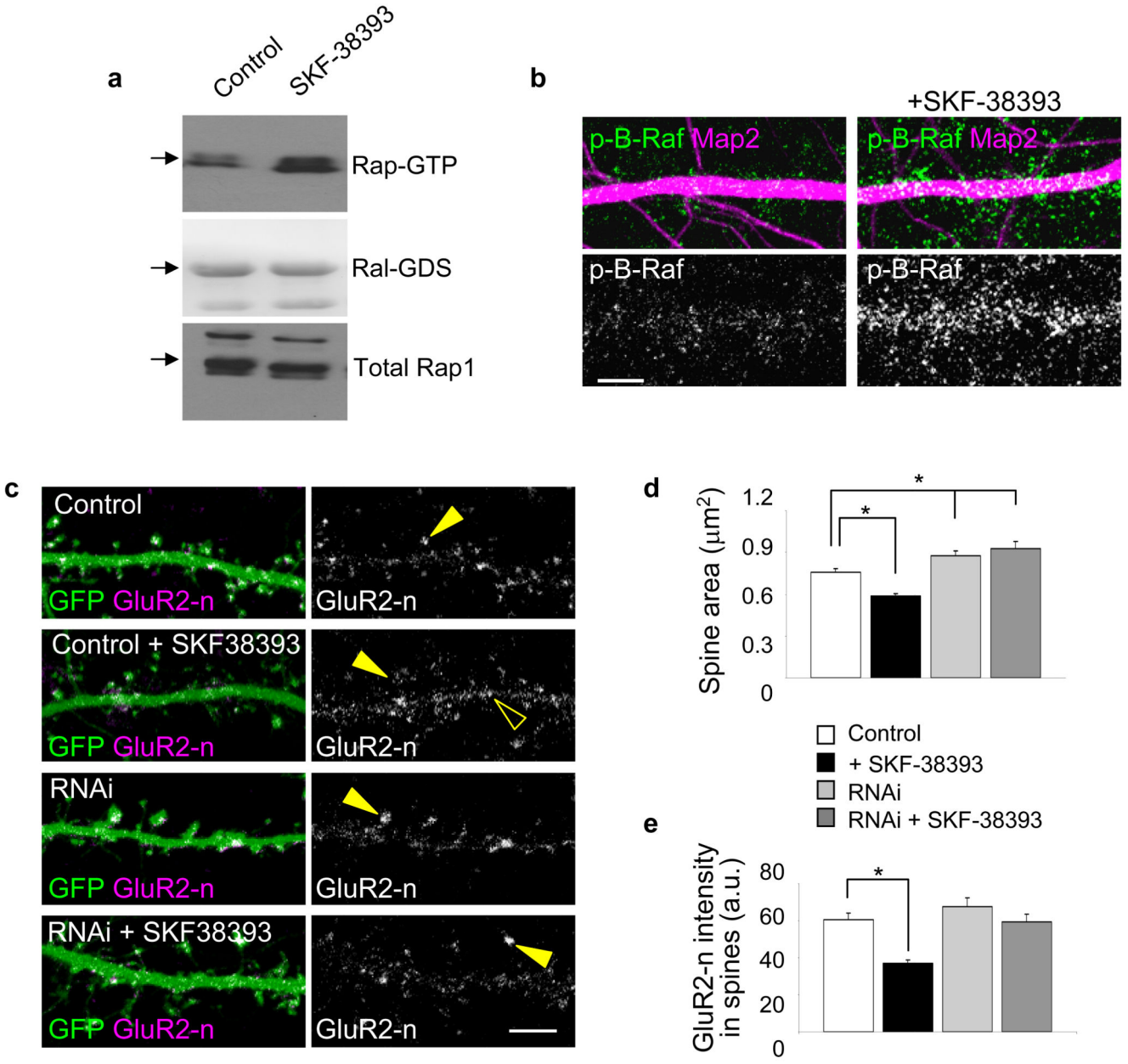

Figure 5.

Dopamine D1/D5-like receptors modulate Rap activity, spine morphology, and GluR2 surface expression. **(a)** Rap activation by SKF-38393 (20 μM, 30 min) in cortical neurons. Fold Rap activation compared to control: 1.62±08 fold increase, *P<0.05, *n* = 4 experiments. **(b)** Effect of SKF-38393 (20 μM, 30 min) on B-Raf phosphorylation *in situ* in dendrites. B-Raf immunofluorescence (a.u.): control, 68.52±4.6; SKF-38393, 141.55±15.2, *P<0.001, *n* = 6–9 cells per condition, 2–3 experiments. **(c)** Effect of SKF-38393 (20 μM, 30 min) on spine morphology and surface GluR2 in spines in cortical neurons (div 28). Epac2 knockdown prevents SKF-38393-dependent spine remodeling and AMPAR removal. GluR2 was detected using an antibody to its extracellular N-terminus (GluR2-n) in non-permeabilized cells. (arrowhead, clusters in spines; open arrowhead, shafts) **(d)**

Quantification of spine areas in e; area (μm^2): control, 0.74±0.02; SKF-38393, 0.59±0.01, Epac2 RNAi, 0.86±0.03; Epac RNAi+SKF-38393, 0.90±0.04, *P<0.001, *n* = 308–426 spines from 9–13 cells per condition, 4 experiments. **(e)** Quantification of surface GluR2 (GluR2-n) clusters in e; GluR2-n immunofluorescence (a.u.): control, 60.6±3.53; SKF-38393, 36.9±1.65; Epac2 RNAi, 67.7±4.48; Epac2 RNAi+SKF-38393, 59.6±3.94, *P < 0.001, *n* = 9–13 cells per condition, 4 experiments. Error bars: s.e.m. Scale bars: 5μm.

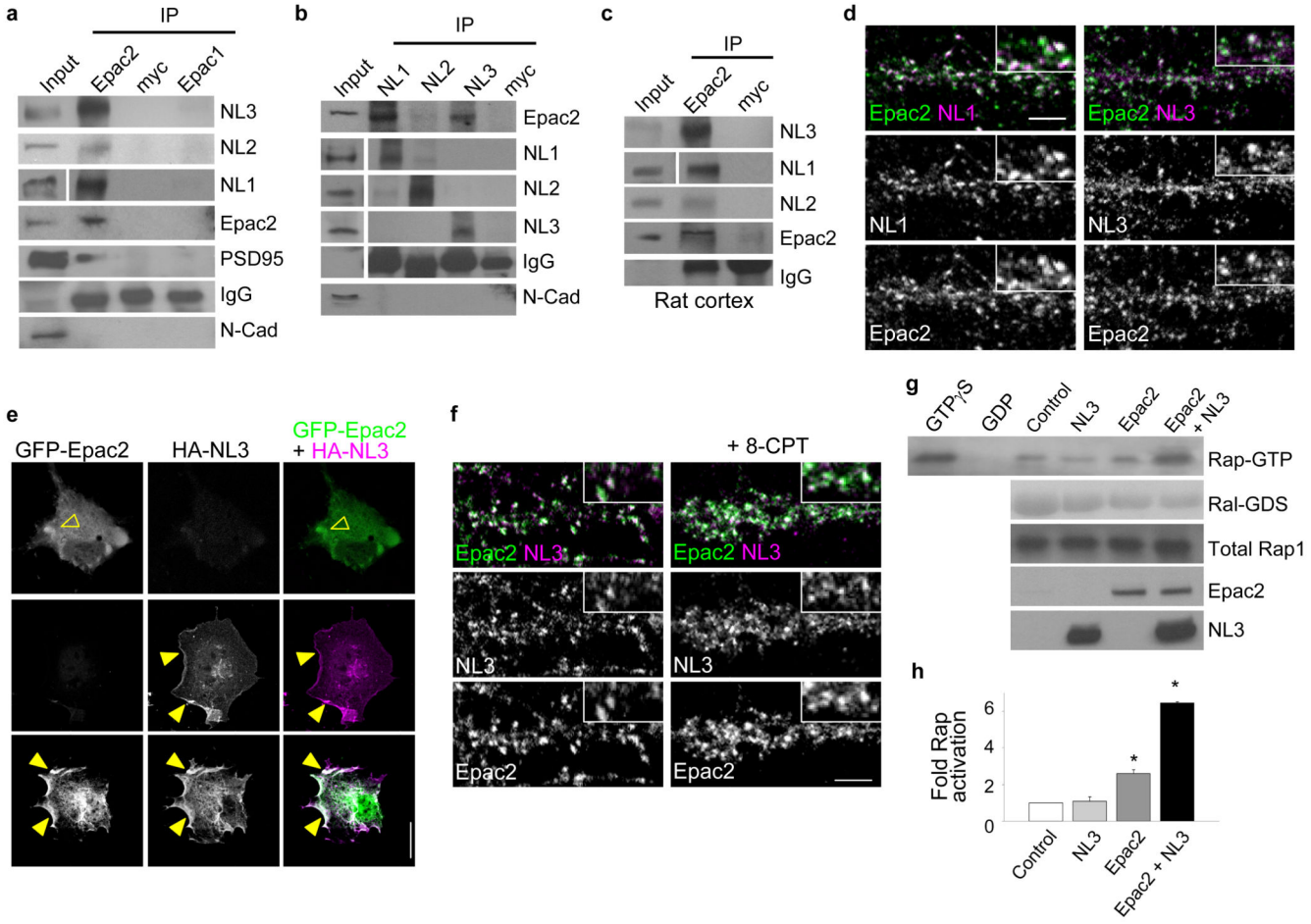

Figure 6.

Epac2 interacts with neuroligins. **(a)** Coimmunoprecipitation of NL1-3 with Epac2 but not Epac1 from cortical neurons (div 28). **(b)** Reverse coimmunoprecipitation of NL1-3 with Epac2 from cortical neurons (div 28). **(c)** Coimmunoprecipitation of Epac2 with NL1–3 from rat forebrain; myc, control antibody. All coimmunoprecipitation experiments were performed 3 times, Western Blots show typical results. **(d)** Immunofluorescence colocalization of Epac2 and NL 1 and 3 on dendrites of cortical pyramidal neurons. **(e)** NL3 affects Epac2 localization. Epitope-tagged Epac2 and NL3 were expressed individually or together in COS7 cells, and visualized by immunostaining. (open arrowhead, cytosolic expression; arrowhead, membrane expression) **(f)** Treatment with 8-CPT (50 μM) increases Epac2/NL3 colocalization along dendrites of mature cortical neurons. Epac2/NL3 colocalized puncta: control, 7.69±0.21; 8-CPT, 11.53±0.58, *P<0.001, *n* = 7–8 cells per condition, 2–3 experiments. **(g)** Coexpression of Epac2 with NL3 in hEK293 cells enhances its Rap-GEF activity. **(h)** Quantification of Rap-GTP in g; fold increase in Rap activity relative to control: NL3, 1.08±0.23, Epac2, 2.61±0.19, NL3+Epac2, 6.45±0.08, *P<0.001, *n* = 3 experiments. Error bars: s.e.m. Scale bars: d, f, 5μm; e 15μm.

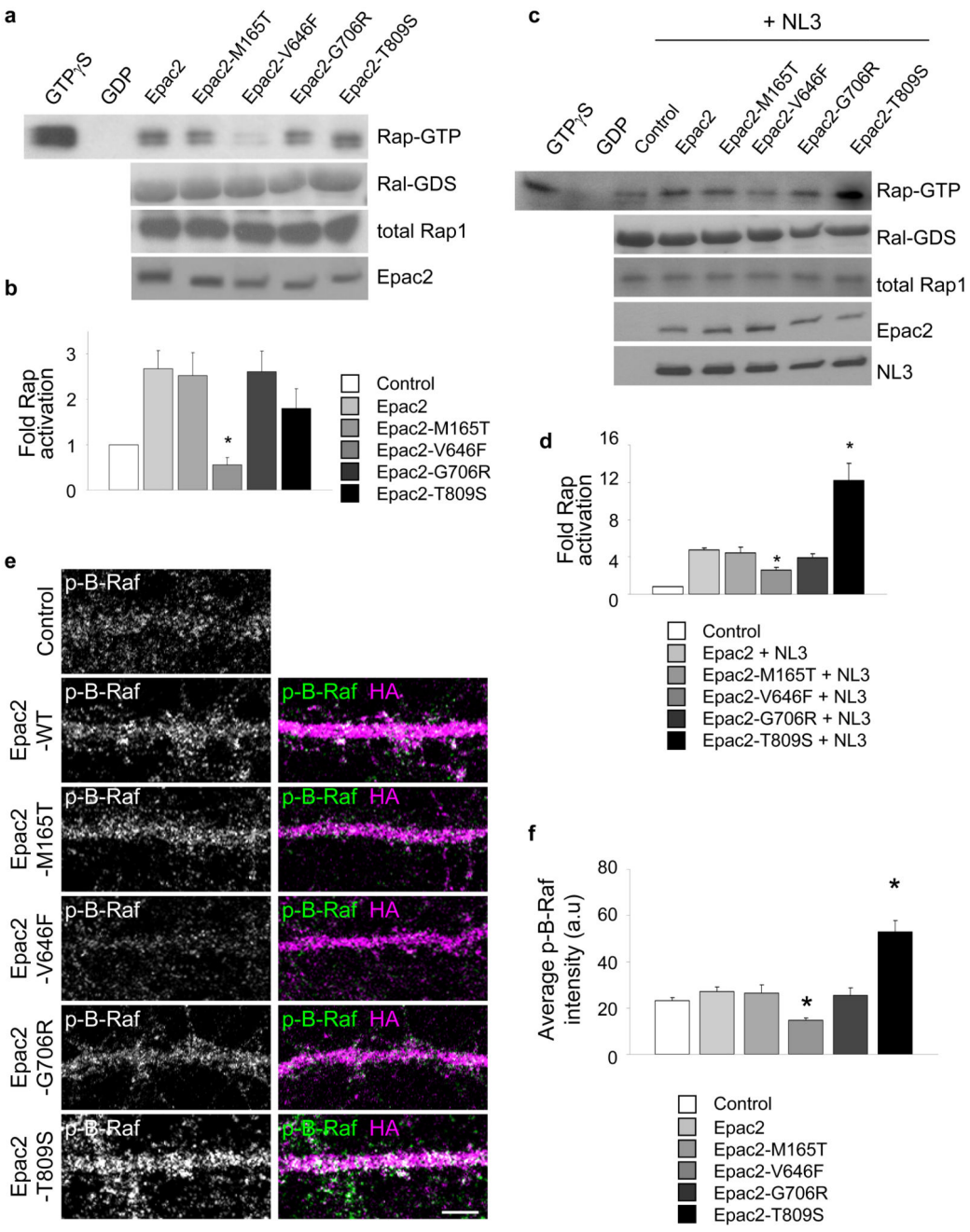

Figure 7.

Disease-associated missense mutations affect Epac2 function. **(a)** Epac2 mutations affected Rap-GEF activity in hEK293 cells transfected with Epac2 or its mutants. **(b)** Quantification of Rap1-GTP in a: reduced Rap1 activation by Epac2-V646F; fold increase in Rap activity relative to control: Epac2-WT, 2.67±0.40, Epac2-M165T, 2.52±0.50, Epac2-V646F, 0.55±0.17, Epac2-G706R, 2.62±0.45, Epac2-T809S, 1.80±0.43, *P<0.01, *n* = 3 experiments. **(c)** Effect of Epac2's missense mutations on NL3-dependent stimulation of its GEF activity. **(d)** Quantification of Rap1-GTP in c: NL3-enhanced Rap activation is reduced

in Epac2-V646F and increased in Epac2-T809S; fold increase in Rap activity relative to control: Epac2-WT, 5.98±0.24, Epac2-M165T, 5.56±0.76, Epac2-V646F, 3.26±0.38, Epac2-G706R, 4.93±0.50, Epac2-T809S, 15.21±2.32, *P<0.001, *n* = 3 experiments. **(e)** Effect of Epac2 mutations on dendritic B-Raf phosphorylation (p-B-Raf) in cortical pyramidal neurons (div 28). **(f)** Quantification of dendritic B-Raf fluorescence intensities in e. Epac2-V646F reduced and Epac2-T809S increased dendritic phospho-B-Raf immunofluorescence; control, 232.2±11.4 Epac2-WT, 272.2±17.3, Epac2-M165T, 265.3±34.2, Epac2-V646F, 145.7±10.5, Epac2-G706R, 255.6±32.0, Epac2-T809S, 528.1±49.5, *P<0.001, *n* = 6–8 cells per condition from 3 experiments. Error bars: s.e.m. Scale bar: 5μm.

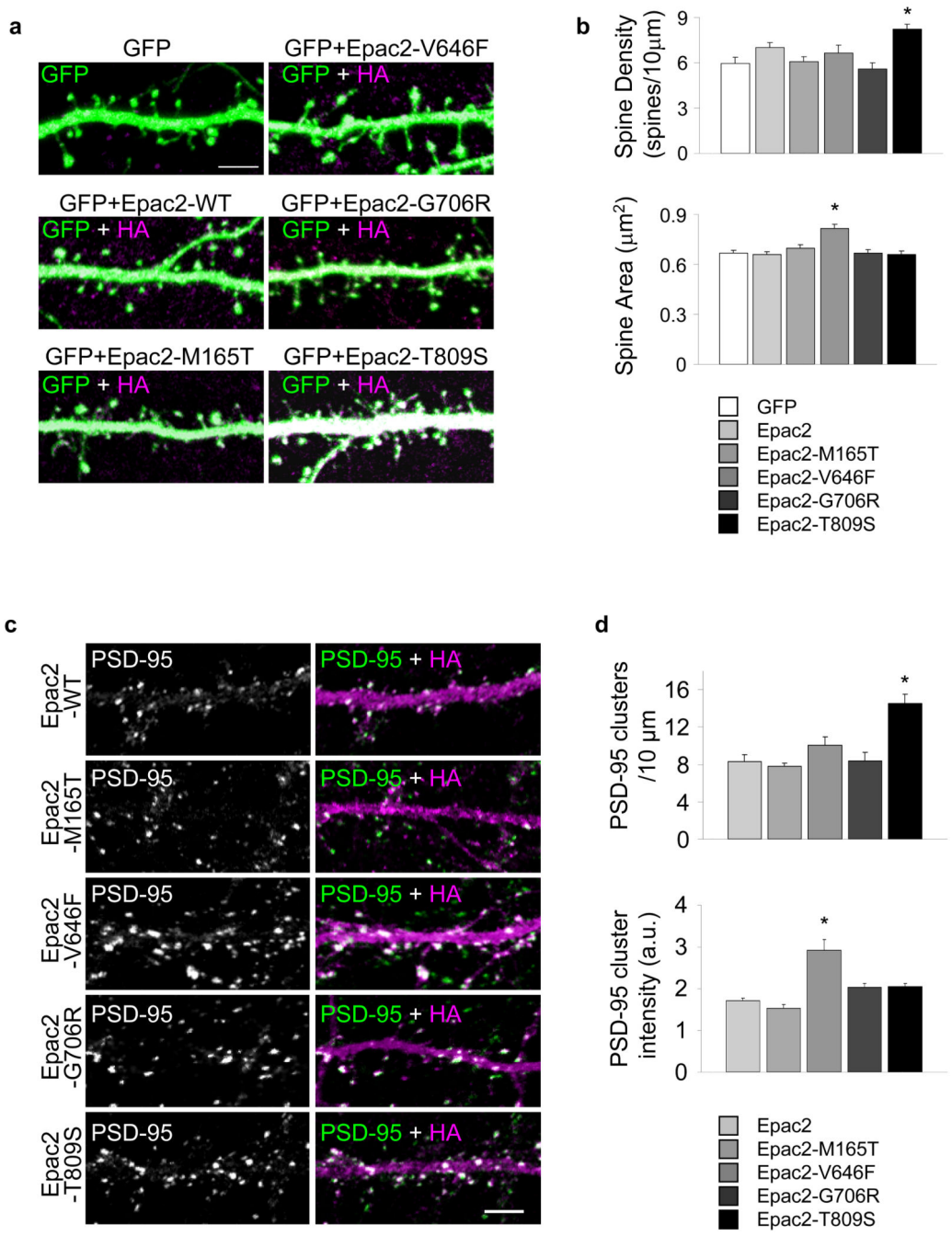

Figure 8.

Epac2 missense mutants affect spine morphology. **(a)** Co-expression of HA-tagged Epac2 or its disease-associated mutants with GFP in cortical pyramidal neurons (div 28); Epac2 mutants Epac2-V646F and Epac2-T809S alter dendritic spine morphology. **(b)** Quantification of the effects on spine area and number in a; area (µm^2): GFP, 0.67±0.02; Epac2-WT, 0.66±0.02; Epac2-M165T, 0.70±0.02; Epac2-V646F, 0.82±0.02; Epac2-G706R, 0.67±0.02; Epac2-T809S, 0.66±0.02, *P<0.001; spines/10µm: GFP, 5.98±0.37; Epac2-WT, 7.00±0.32; Epac2-M165T, 6.07±0.34; Epac2-V646F, 6.66±0.52; Epac2-G706R, 5.60±0.40;

Epac2-T809S, 8.23±0.31, *P<0.001, *n* = 406-592 spines from 9 cells per condition, 4 experiments. **(c)** Effects of expression of HA-Epac2 mutations on the average intensity and number of endogenous PSD-95 immunofluorescent puncta in dendrites. **(d)** Quantification of average immunofluorescence intensity and linear density of PSD-95 puncta in c. Epac2-V646F increased PSD-95 average intensity in individual puncta (a.u.); Epac2-WT, 170.5±7.07; Epac2-M165T, 152.4±9.16; Epac2-V646F, 291.0±26.0; Epac2-G706R, 203.7±8.24; Epac2-T809S, 205.3±7.46, *P<0.001. Epac2-T809S increased the number of PSD-95 clusters: Epac2-WT, 8.26±0.76; Epac2-M165T, 7.80±0.29; Epac2-V646F, 10.05±0.93; Epac2-G706R, 8.34±0.98; Epac2-T809S, 14.5±1.01, *P<0.001, *n* = 4–8 cells, 2–3 experiments. Error bars: s.e.m. Error bars: s.e.m. Scale bars: 5μm.